ChemComm

Electrodeposited nickel and gold nanoscale metal meshes with potentially interesting photonic properties

Lianbin Xu,[ab] Weilie L. Zhou,[b] Christoph Frommen,[b] Ray H. Baughman,[c] Anvar A. Zakhidov,[c] Leszek Malkinski,[b] Jian-Qing Wang[b] and John B. Wiley*[ab]

[a] *Department of Chemistry, University of New Orleans, New Orleans, LA 70148-2820, USA. E-mail: jwiley@uno.edu*
[b] *Advanced Materials Research Institute, University of New Orleans, New Orleans, LA 70148-2820, USA*
[c] *Honeywell Int., Corporate Technology, Morristown, NJ 07962-1021, USA*

Received (in Irvine, CA, USA) 11th January 2000, Accepted 14th April 2000
Published on the Web 22nd May 2000

Nickel and gold meshes having three-dimensional periodicity at optical wavelengths and nanoscale structural fidelity have been prepared by electrodeposition within close-packed silica sphere arrays.

There is major current interest in the fabrication of nanoporous metal arrays.[1–4] Routine access to such materials could impact a variety of areas including photonics, magnetics, catalysis, electrochemical applications and thermoelectrics. Recent reports have described the formation of 3-D metal meshes within colloidal silica or polymer membranes through the use of molten metal infiltration, nanoparticle infiltration and electroless methods.[4–6] Though metal electrodeposition methods have been effectively used for membranes with one-dimensional pore structures,[7] the extension of this technique to three-dimensional structures has not been reported. This electrochemical method has the major advantage of readily producing well defined metal meshes of materials melting at such high temperatures that melt infiltration is prohibited by template structural instability. Herein, we describe the use of this approach for the fabrication of nickel and gold arrays having three-dimensional periodicity at optical wavelengths.

Silica membranes (opal) were prepared by published methods.[8] Silica spheres with a diameter of *ca.* 300 nm diameter were initially prepared from tetraethylorthosilicate (TEOS). The spheres were then formed into close-packed lattices through a sedimentation process over several months. This precipitate was then sintered at 120 °C for two days and then 750 °C for 4 h, producing a robust opalescent piece that could be readily cut into smaller sections. Electrodes were formed from the opal (typically 7 × 10 × 1.5 mm) by first depositing *ca.* 0.5 μm thick copper films on one side of the piece by magnetron sputtering. A length of wire was attached to the copper backing with silver paste (Ted Pella, Inc.) and the copper/wire side of the electrode, as well as the edges, were sealed off with neoprene glue (Elmer's). For metal deposition, the electrodes were immersed into nickel or gold plating solutions (Technic, Inc.) with a platinum wire counter electrode. Electrodeposition was carried out by a constant current method over a 36 h period; a low current density (0.50 mA cm^{-2}) was used in an effort to achieve even deposition within the opal membrane. Low current densities such as that used here have been found to be effective in the growth of nanowires. After deposition, the opal was washed thoroughly with distilled water and the neoprene layer peeled off. To remove the silica matrix, the metal–opal pieces were soaked in a 2% HF solution for 24 h. This resulted in a dark opalescent metal membrane (*ca.* 100 μm thick). Scanning electron micrographs (SEM) were obtained on a JEOL JSM 5410 SEM. Magnetic measurements on the nickel mesh were performed on a Quantum Design MPMS-5S SQUID susceptometer. The mesh was fixed between two pieces of Kapton tape and placed in a commercially available soda straw. No correction for the diamagnetic contribution of the sample holder was taken into account because it was by at least three orders of magnitude smaller than the response generated from the Ni-mesh. The field dependence was studied at various temperatures (2, 10 and 300 K) in external fields up to ±5 T. The temperature dependence was measured in a zero-field cooled (zfc) and a field-cooled (fc) cycle at 1000 G.

This electrodeposition method produces well-defined metal meshes. Fig. 1(a) shows a cross-section of the closed-packed silica membrane (10 000× magnification). Stacking faults are present on (111) planes in the original opal, which will be replicated in the metal mesh. Electrodeposition fills the void space between the close-packed spheres. Fig. 1(b) shows a section of a nickel metal mesh (10 000×) after dissolution of the silica spheres. This image highlights the packing variation for these spheres. Different sections corresponding to (111), (100) and (110) orientations can be observed. Fig. 2(a) and (b) are views of predominately the (100) and the (110) planes, respectively. Fig. 2(c) is a higher magnification (50 000×) of the (100) plane. The square features are essentially cubes with concave sides that arise from filling the octahedral sites in the close-packed structure. Each cube is connected to eight other cubes through its vertices *via* tetrahedra [Fig. 2(d)]. The structure is akin to the fluorite structure (CaF_2) where the calcium ions, representing the cubes, are eight coordinate and the fluoride ions, representing the tetrahedra, are four coordinate. Based on the diameter of the closed-packed spheres of *ca.* 300 nm, one would predict minimum diameters of *ca.* 50, 70 and 120 nm for the interconnects, tetrahedra and cubes, respectively, as is observed. Since the metal mesh crystals are interpenetrating air- and metal-phase networks, they are

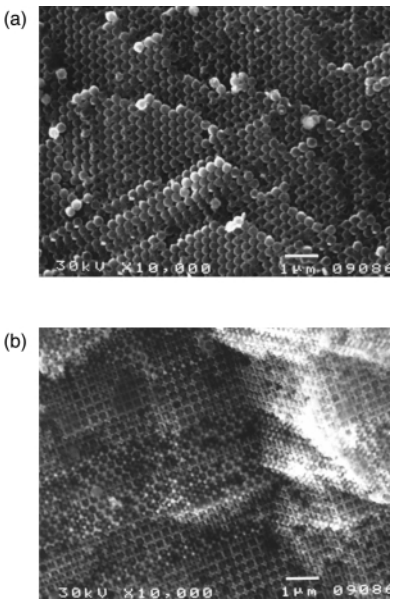

Fig. 1 (a) Scanning electron micrograph of a silica opal piece at 10 000× in the (111) plane. (b) Electrodeposited nickel mesh after dissolution of the opal membrane (10 000×).

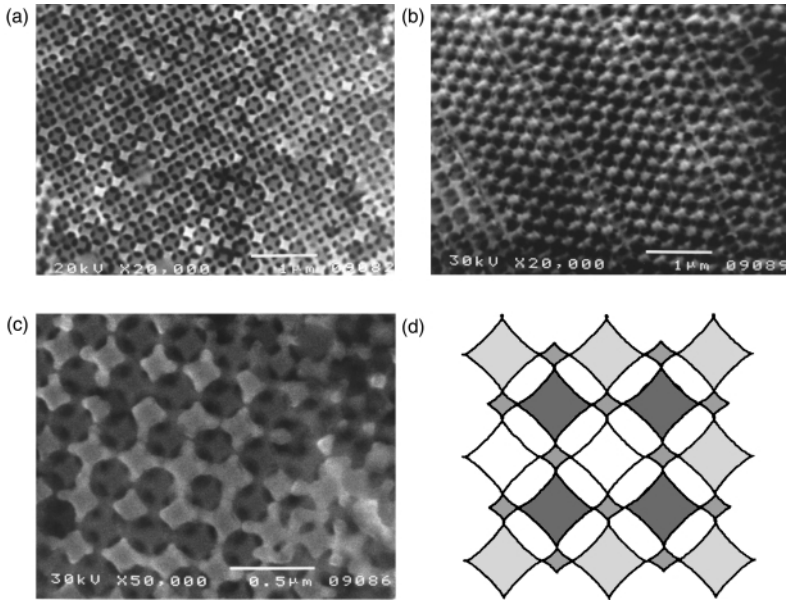

Fig. 2 SEM photographs of (a) nickel metal mesh along the 100 direction, (b) gold mesh predominately along the 110 direction, (c) 50 000× magnification of square nickel mesh and (d) illustration of square motif seen in (c) (the lighter regions are closer and the darker regions are progressively further away).

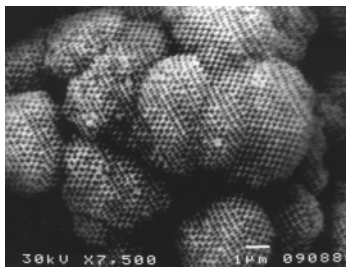

Fig. 3 SEM photograph showing the spherical morphology of the gold mesh (7500×).

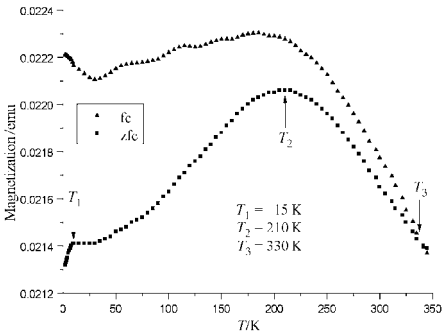

Fig. 4 Zero-field cooled (zfc), field-cooled (fc) cycle in an external field of 1000 G for the electrodeposited Ni-mesh after removal of the opal matrix.

metallo-dielectric photonic crystals, which are predicted to have an unusual metallicity bandgap.[1]

Interestingly, the extended nickel metal arrays maintain their structure after removal of the silica membrane, while the gold arrays appear to collapse in on themselves. Fig. 3 shows a low magnification image (7500×) of gold. Some areas of the mesh appear spherical in what look like 'florets'; localized structural features, however, are still quite apparent between the regions. Though this effect may simply be due to incomplete filling during electrodeposition, it is also possible that it may be associated with the greater malleability of gold relative to that of nickel. A possibly related effect has recently been described by Jiang *et al.*,[6] who reported curling of gold films made by the electroless method.

Magnetic measurements on the nickel mesh show size effects due to the nanometer dimensions of the components. The material exhibited a coercive field (H_c) of 500 G at 2 K that decreased slightly with increasing temperature (H_c = 300 G at 300 K). This value is much higher than that found in bulk nickel, which is on the order of a few tens of G. Such an enhancement in the coercivity is well known for other size-constrained magnetic systems.[9] The presently observed coercive field is about four times smaller than reported for 53 nm diameter electrodeposited Ni wires[10] (2000 G at T = 5 K), which is possibly due to the absence of a 'true' quantum confinement and/or structural disorder. The temperature dependence of the magnetization (Fig. 4) shows a sharp inflection at 15 K, a broad inflection at 210 K and a merging of the fc and zfc curves at 330 K. It is not clear at this point how these features relate to the combined superparamagnetic effects of the components in the metal meshes, interconnects, tetrahedra and cubes. Micromagnetics calculations may give some insight into the response of these arrays.

We gratefully acknowledge support from the Department of Defense (DARPA MDA972-97-1-0003 and DAA-96-J-036).

Notes and references

1 D. F. Sievenpiper, M. E. Sickmiller and E. Yablonovitch, *Phys. Rev. Lett.*, 1996, **76**, 2480; D. F. Sievenpiper, E. Yablonovitch, J. N. Winn, S. Fan, P. R. Villeneuve and J. D. Joannopoulos, *Phys. Rev. Lett.*, 1998, **80**, 2829.
2 M. P. Hogarth, J. Munk, A. K. Shukla and A. J. Hamnett, *Appl. Electrochem.*, 1994, **24**, 85.
3 J. Kleperis, G. Vaivars, A. Vitins, A. Lusis and A. Galkin, *NATO ASI Ser. 3* (New Promising Electrochemical Systems for Rechargeable Batteries), 1996, **6**, 285.
4 R. H. Baughman, A. A. Zakhidov, I. I. Khayrullin, I. A. Udod, C. Cui, G. U. Sumanasekera, L. Grigorian, P. C. Eklund, V. Browning and A. Ehrlich, *Proc. Intl. Conf. Thermoelectrics (ICT'98)*, Nagoya, Japan, 1998.
5 O. D. Velev, P. M. Tessier, A. M. Lenhoff and E. W. Kaler, *Nature*, 1999, **401**, 548.
6 P. Jiang, J. Cizeron, J. F. Bertone and V. L. Colvin, *J. Am. Chem. Soc.*, 1999, **121**, 7957.
7 C. R. Martin, *Chem. Mater.*, 1996, **8**, 1739 and references therein.
8 N. D. Deniskina, D. V. Kalinin and L. K. Kazantseva, *Gem Quality Opals: Synthetic and Natural Genesis*, Nauka, Novosibirsk, 1987 (in Russian); A. P. Philips, *J. Mater. Sci. Lett.*, 1987, **8**, 1371; P. J. Darragh, A. J. Gaskin and J. V. Sanders, *Sci. Am.*, 1976, **234**, 84.
9 B. D. Cullity, *Introduction to Magnetic Materials*, Addison-Wesley Publishing, Reading, MA, 1972, p. 383 and references therein.
10 J. Meier, B. Doudin and J.-Ph. Ansermet, *J. Appl. Phys.*, 1996, **79**, 6010.